Supporting Information

Molecular mechanism of mechanical breathing in organic mixed ionic-electronic conductors

Xixian Yang[†], Hong Sun[†,‡], Xiaomei He[†], Kejie Zhao[†,*]

[†]School of Mechanical Engineering, Purdue University, West Lafayette, IN 47907, United States

[‡]Physics Division, Lawrence Livermore National Laboratory, Livermore, CA 94550, United States

*Corresponding author. kjzhao@purdue.edu (K. Z.)

Table S1. Selected electrolytes for studying the effects of ion concentration, organic solvents, and anions on the swelling behavior of OMIECs.

Electrolytes	Effect of ion concentrations	Effect of organic solvents	Effect of anions
1.0 M $LiBF_4$ in PC			✓
0.2 M $LiClO_4$ in PC	✓		
1.0 M $LiClO_4$ in PC	✓		✓
1.0 M $LiPF_6$ in EC/DEC		✓	
1.0 M $LiPF_6$ in PC		✓	✓
1.0 M LiTFSI in PC			✓

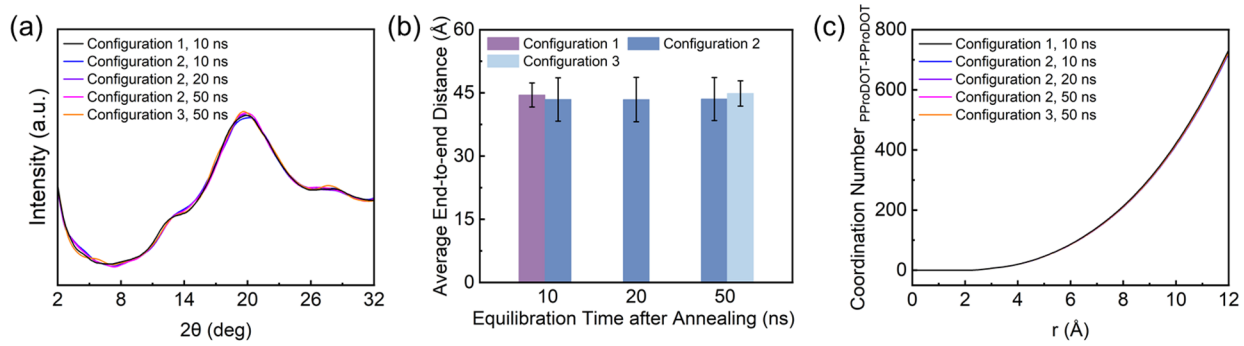

Figure S1. Structural characterization of self-aggregated PProDOT generated from three different initial configurations. Specific equilibration protocol for each configuration is described in the Methodology section. (a) Calculated XRD patterns. (b) Average end-to-end distances. (c) Cumulative coordination numbers between PProDOT atoms.

In figure S1, the equilibrium state is confirmed for the three self-aggregated PProDOT models by examining the XRD patterns, coordination numbers as well as the end-to-end distances. Specifically, configurations 1 and 2 equilibrated for 10 ns after thermal annealing have highly comparable XRD patterns, average end-to-end distances, and coordinate numbers. In configuration 2, the structural characteristics are overlapped for the 10 ns, 20 ns, and 50 ns equilibration after thermal annealing. Moreover, in configuration 3, the repeated thermal annealing and extended equilibration of 50 ns do not make any difference in the XRD pattern, end-to-end distance, and coordination number compared to configurations 1 and 2. These calibrations indicate that 10 ns equilibration after thermal annealing is sufficient to generate the self-aggregated PProDOT at equilibrium state.

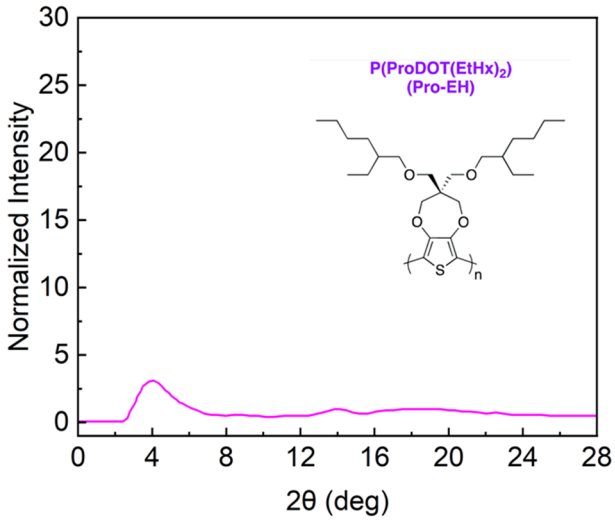

Figure S2. Linecut along the Q_z direction from the GIWAXS image of charge-neutral PProDOT[1]. Reproduced from [1]. Copyright [2020] American Chemical Society.

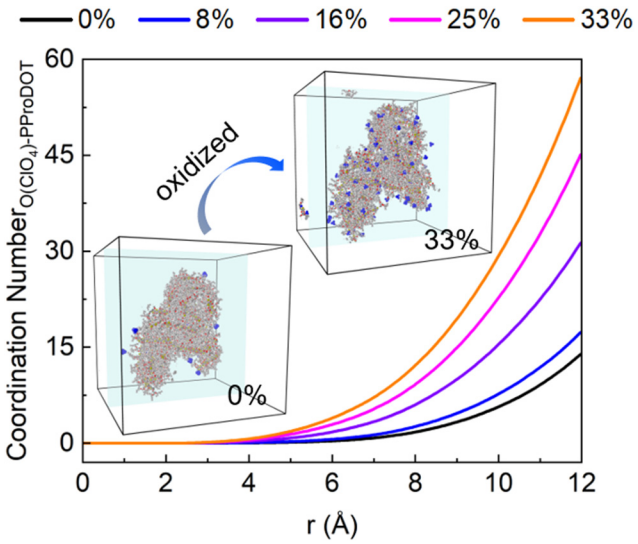

Figure S3. Cumulative coordination numbers (CNs) between O in ClO_4^- and PProDOT in 1.0 M $LiClO_4$ in PC at different oxidation states. Inset figures show the MD snapshots where only PProDOT and ClO_4^- anions within 3.5 Å to PProDOT are shown. The cross sections of the sliced simulation boxes are shown to illustrate the ClO_4^- absorption into PProDOT.

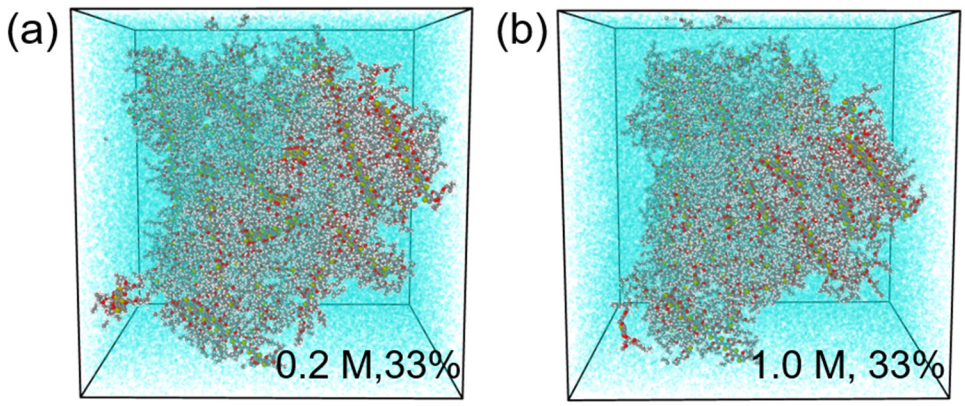

Figure S4. MD snapshots showing the equilibrated state of PProDOT soaked in (a) 0.2 M and (b) 1.0 M $LiClO_4$ in PC. Li^+ and ClO_4^- are not shown for better illustration of mechanical swelling of PProDOT.

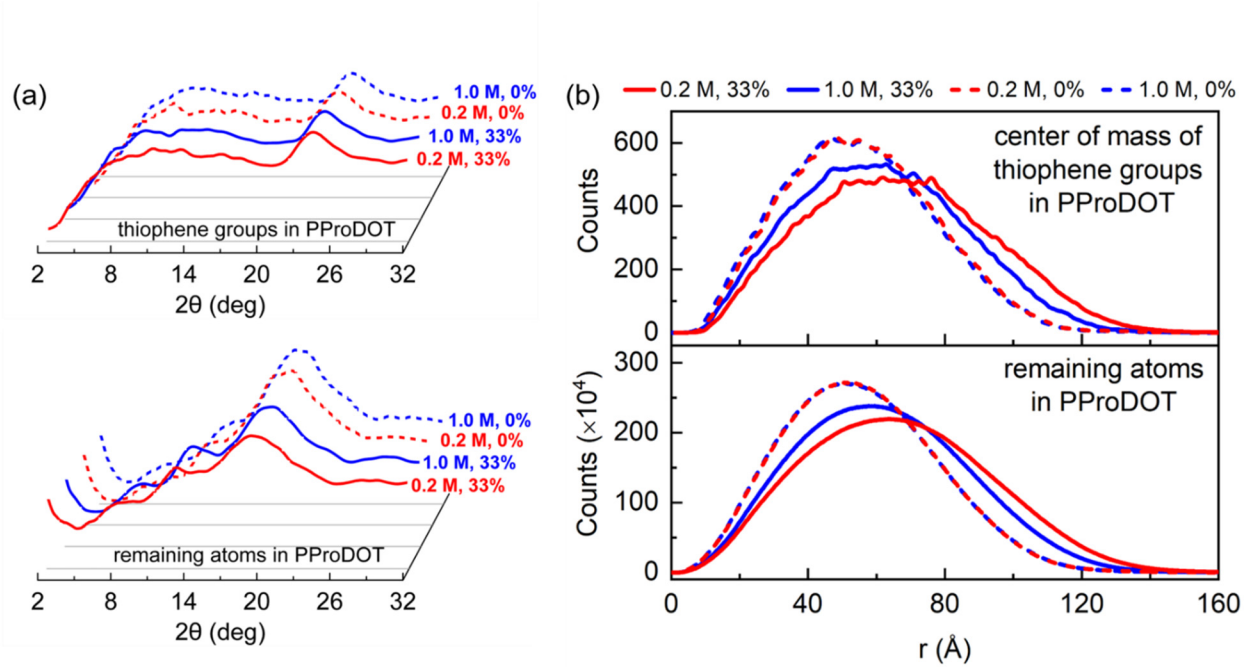

Figure S5. Comparison of the structural characteristics of PProDOT in 0.2 M and 1.0 M $LiClO_4$ in PC. (a) Calculated XRD patterns of the thiophene groups (upper panel) and the remaining atoms (lower panel) in PProDOT. (b) Differential CNs of the center of mass (COMs) of the thiophene groups (upper panel) and the remaining atoms (lower panel) in PProDOT at two different oxidation states.

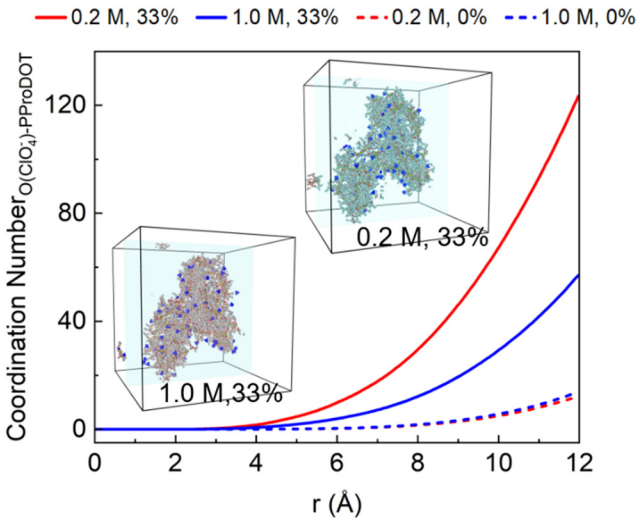

Figure S6. Cumulative CNs between O in ClO_4^- and PProDOT in the electrolytes of 0.2 M and 1.0 M $LiClO_4$ in PC. Inset figures show the MD snapshots where the neighboring environment between PProDOT and ClO_4^- anions within 3.5 Å to PProDOT are shown.

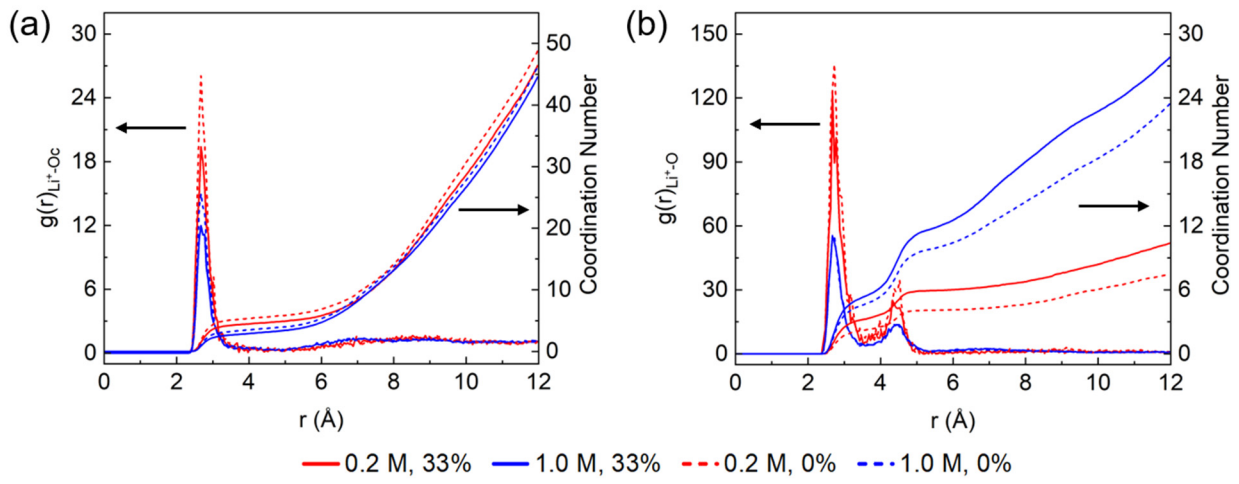

Figure S7. Changes of the solvation structure in the electrolytes of 0.2 M and 1.0 M $LiClO_4$ in PC upon oxidation of PProDOT. (a) RDF and cumulative CNs between Li^+ and Oc in PC. (b) RDF and cumulative CNs between Li^+ and O in ClO_4^-.

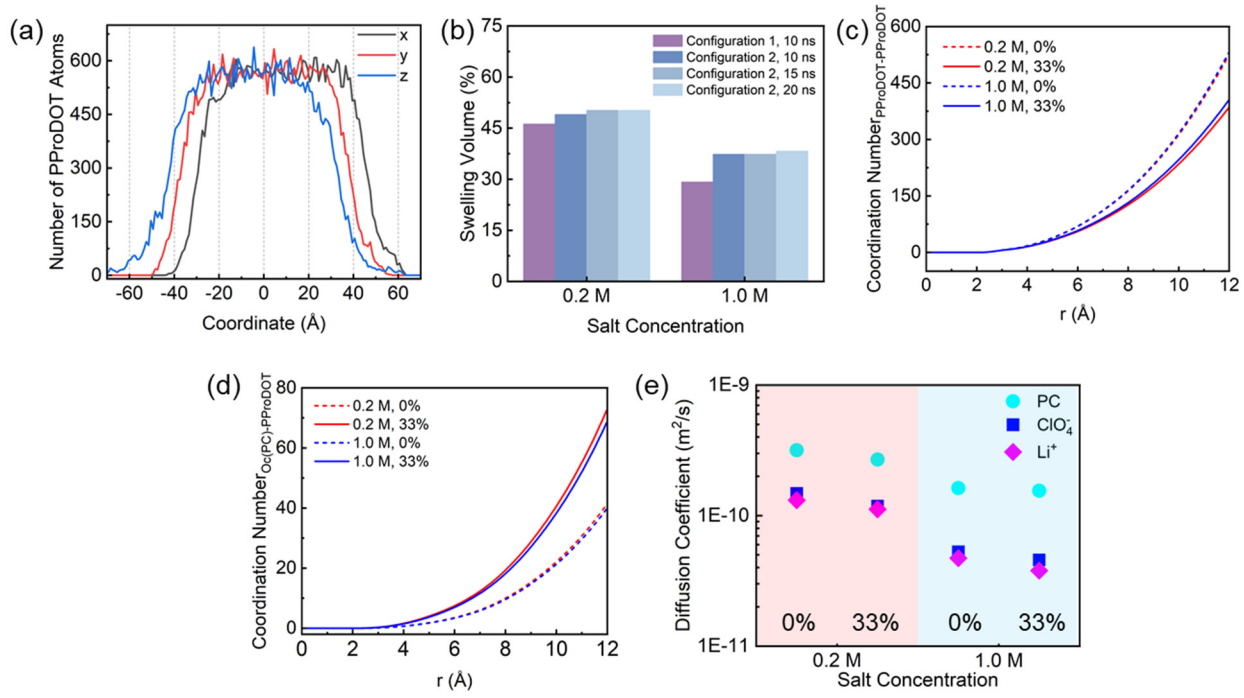

Figure S8. Effects of salt concentration using a different initial PProDOT configuration (configuration 2), where self-aggregated PProDOT is soaked in electrolytes with different placement positions of ions and solvent. (a) Number density profiles of PProDOT atoms along the *x*, *y,* and *z* directions. (b) Comparison of the calculated swelling volumes of PProDOT in 0.2 M and 1.0 M $LiClO_4$ in PC using models with different initial configurations subject to various equilibration times. (c) Cumulative coordination numbers between PProDOT atoms at charge-neutral (0%) and oxidized (33%) states. (d) Cumulative coordination numbers between Oc in PC and PProDOT at charge-neutral (0%) and oxidized (33%) states. (e) Diffusion coefficients of PC, ClO_4^-, and Li^+ with two different salt concentrations when PProDOT is at the charge neutral (0%) and oxidized (33%) states.

To validate the modeling protocol and ensure the reproducibility of the simulation results, we use models of distinct initial configurations to study the effect of salt concentration with

extended equilibration time from 10 ns to 20 ns. Details about the models can be found in the Methodology section.

The number density profiles of PProDOT are plotted along the *x*, *y*, and *z* directions (Figure S8a). The reference box is then identified according to the plateaus from -14.5 Å to 38.5 Å in the *x* direction, from -25.5 Å to 26.5 Å in the *y* direction, and from -28.5 Å to 14.5 Å in the *z* direction, which significantly differ from the -20 Å to 20 Å range in all the three directions in configuration 1 as discussed in the main text. Despite the distinct reference volume, the calculated swelling volumes of PProDOT are very close to those displayed in the main text (which are also shown in purple in Figure S8b), which corroborates with the finding that PProDOT swells more in the dilute electrolyte. Besides, the differences in swelling volume using 15 ns and 20 ns equilibration are all less than 1%, compared to the 10 ns equilibration process, in both electrolytes. The coordination number analysis, including the coordination numbers between PProDOT atoms (Figure S8c) and those between Oc in PC and PProDOT (Figure S8d) further supports the swelling volume results and is consistent with Figure 8b. The consistency is also observed for diffusion coefficients between Figure S8e and Figure 8c. The agreement of simulation results obtained from different initial configurations validate the equilibration protocol and prove the reproducibility of the results.

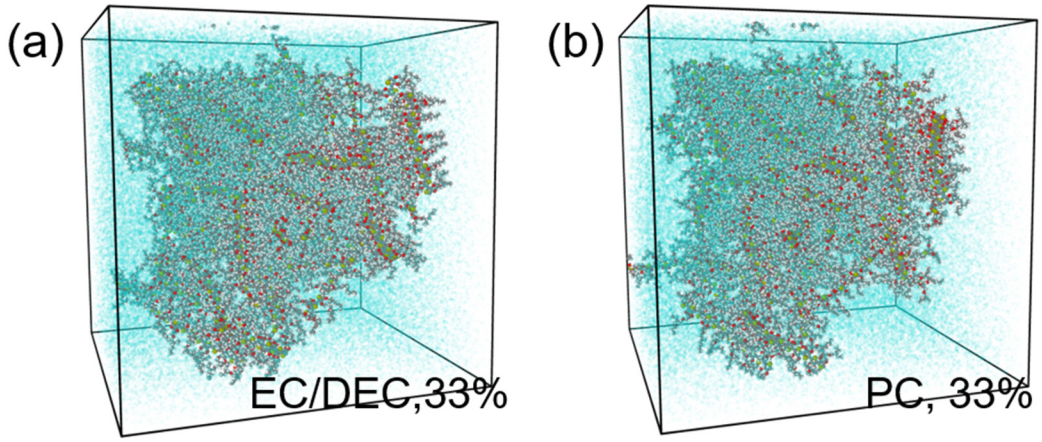

Figure S9. MD snapshots of the final equilibrated states of PProDOT in the electrolytes of EC/DEC and PC solvents. The charge species including Li^+ and PF_6^- are not shown for better illustration of the swelling of PProDOT.

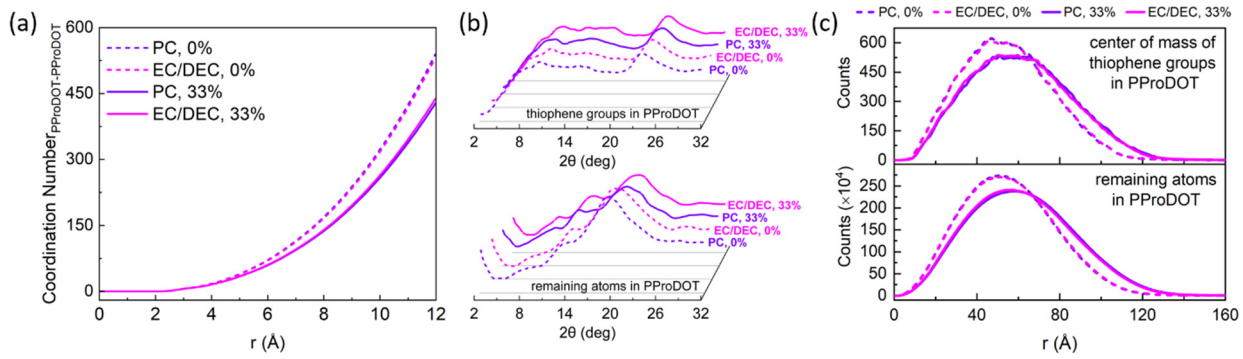

Figure S10. Comparison of structural characteristics of PProDOT in the electrolytes of 1.0 M $LiPF_6$ in PC and EC/DEC. (a) Cumulative CNs between PProDOT atoms. (b) Calculated XRD patterns of the thiophene groups (upper panel) and the remaining atoms (lower panel) in PProDOT. (c) Differential CNs of COMs of the thiophene groups (upper panel) and the remaining atoms (lower panel) in PProDOT without considering those from the same chain.

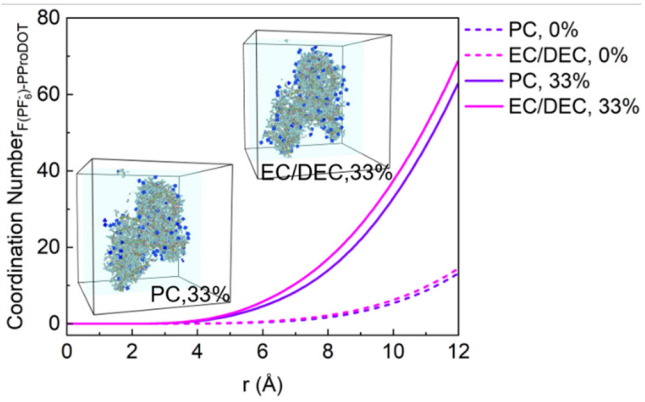

Figure S11. Cumulative CNs between F in PF_6^- and PProDOT in the electrolytes of 1.0 M $LiPF_6$ in PC and EC/DEC. Inset figures are MD snapshots where PProDOT and the PF_6^- anions within 3.5 Å to PProDOT are shown.

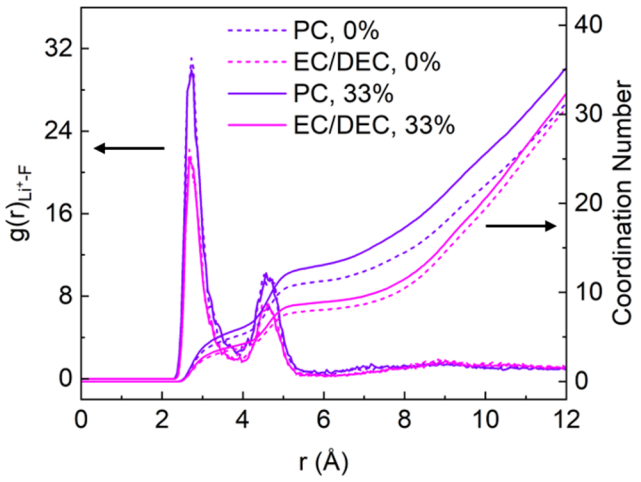

Figure S12. Comparison of RDF and cumulative CNs between Li^+ and F in PF_6^- in the electrolytes of 1.0 M $LiPF_6$ in PC and EC/DEC.

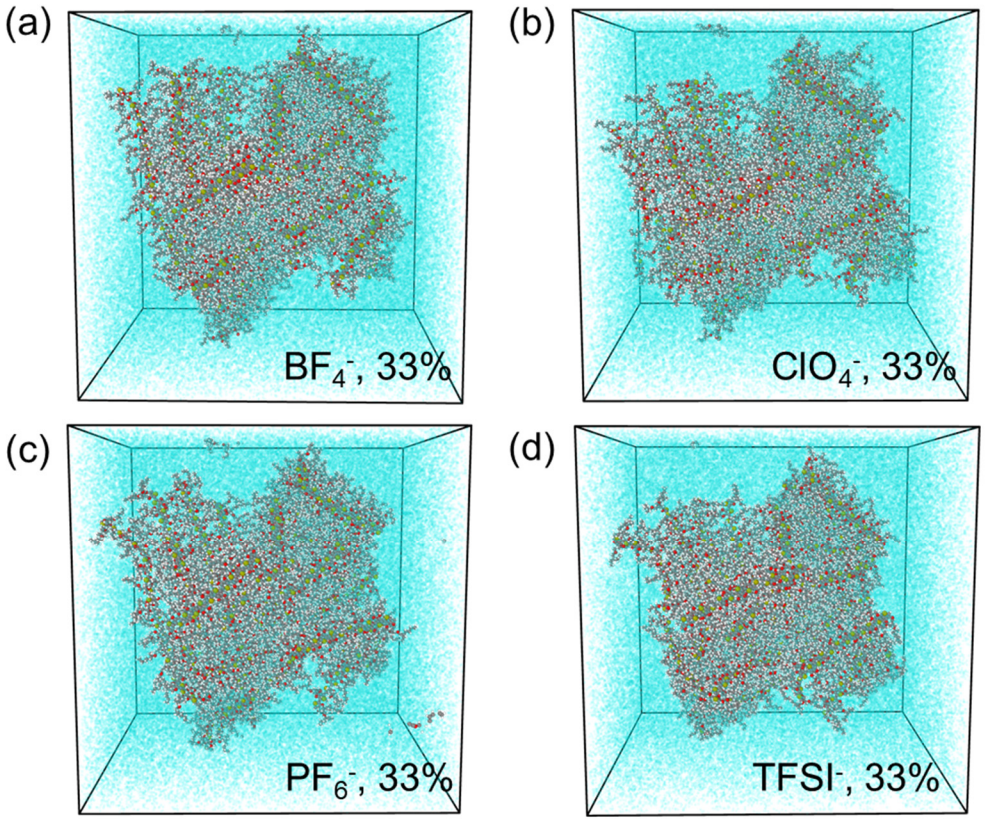

Figure S13. MD snapshots of the final equilibrated state of PProDOT in the electrolytes of 1.0 M $LiBF_4$, $LiClO_4$, $LiPF_6$, and LiTFSI in PC. The absorbed ions including Li^+ and anions are not included for better illustration of the swelling of PProDOT.

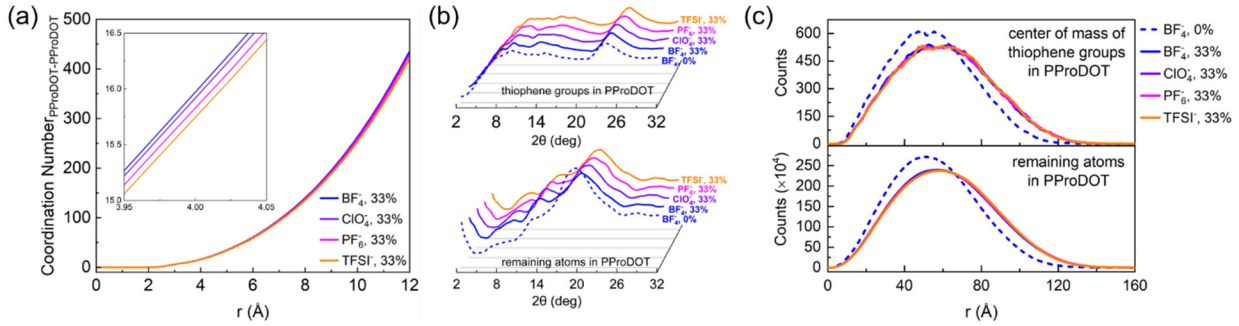

Figure S14. Structural characteristics of PProDOT in the electrolytes of 1.0 M $LiBF_4$, $LiClO_4$, $LiPF_6$, and LiTFSI in PC. (a) Cumulative CNs between PProDOT and PProDOT at the oxidation level of 33%. The inset figure is an enlarged view of the CNs. (b) Calculated XRD patterns of the thiophene groups (upper panel) and the remaining atoms (lower panel) in PProDOT. (c) Differential CNs of COMs of the thiophene groups (upper panel) and the remaining atoms (lower panel) in PProDOT excluding those from the same chain.

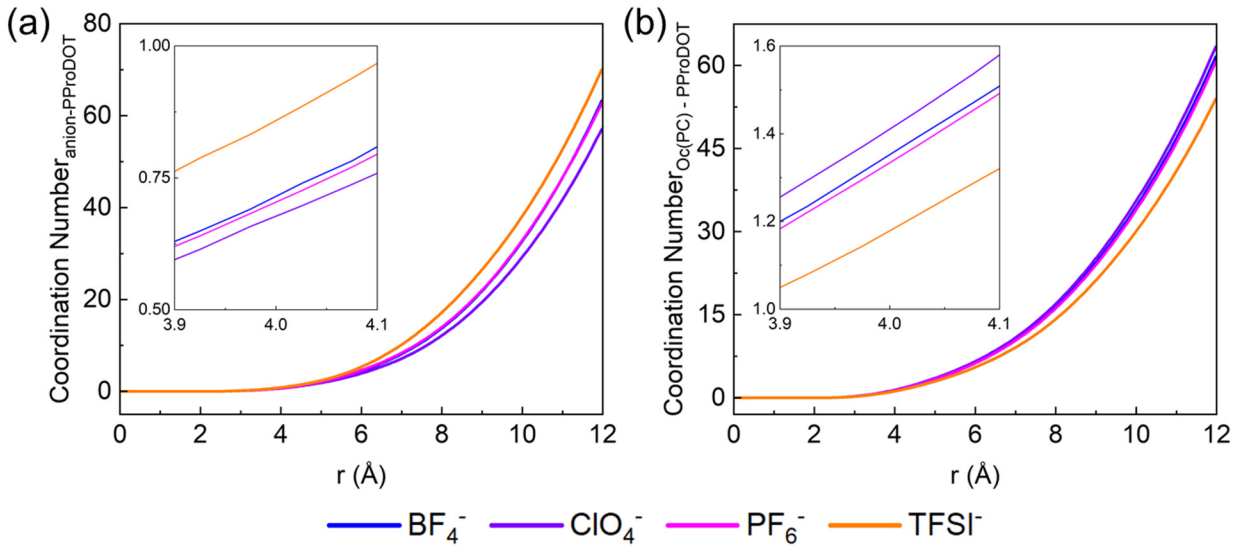

Figure S15. (a) Cumulative CNs between the anion (F in BF_4^-, O in ClO_4^-, F in PF_6^-, and O in $TFSI^-$) and PProDOT at the oxidized state (33%) in the four different electrolytes. (b) Cumulative CNs between Oc in PC and PProDOT.

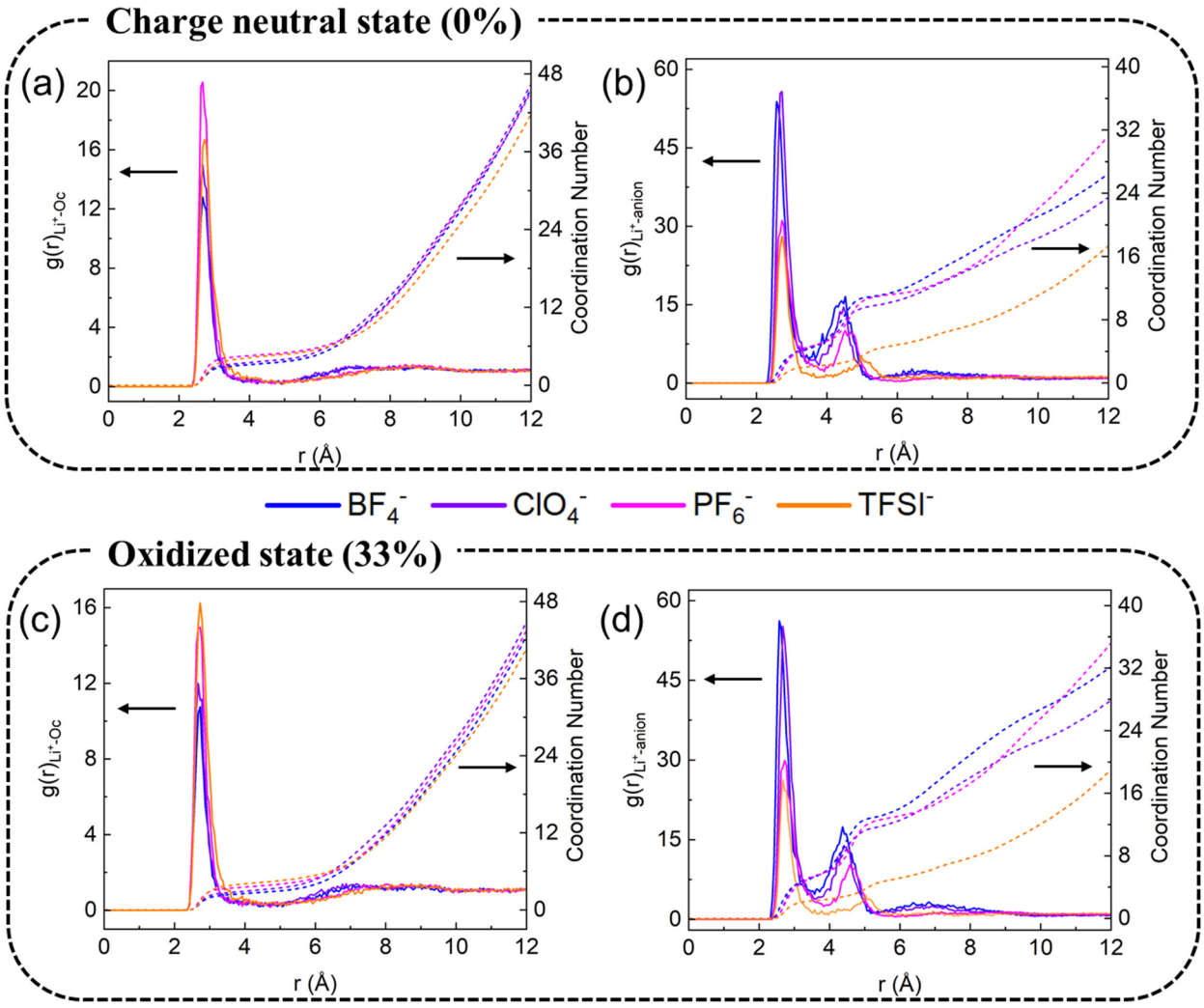

Figure S16. Solvation structure analysis in the electrolytes of 1.0 M $LiBF_4$, $LiClO_4$, $LiPF_6$, and LiTFSI in PC at two oxidation states of PProDOT. Cumulative CNs (a) between Li^+ and Oc in PC and (b) between Li^+ and anion (F in BF_4^-, O in ClO_4^-, F in PF_6^-, and O in $TFSI^-$) at the charge neutral state (0%). Cumulative CNs (c) between Li^+ and Oc in PC and (d) between Li^+ and anion (F in BF_4^-, O in ClO_4^-, F in PF_6^-, and O in $TFSI^-$) at the oxidized state (33%).

Reference

(1) Pittelli, S. L.; Keersmaecker, M. D.; Jr, J. F. P.; Österholm, A. M.; Ochieng, A. M.; Reynolds, J. R. Structural Effects on the Charge Transport Properties of Chemically and Electrochemically Doped Dioxythiophene Polymers. *J. Mater. Chem. C* **2020**, *8* (2), 683–693. DOI: 10.1039/C9TC05697A